

Deepfake Detection via Knowledge Injection

Tonghui Li Yuanfang Guo Heqi Peng Zeming Liu Yunhong Wang
School of Computer Science and Engineering, Beihang University, China

lthlth, AndyGuo, penghq, zmliu, yhwang@buaa.edu.cn

Abstract

Deepfake detection technologies become vital because current generative AI models can generate realistic deepfakes, which may be utilized in malicious purposes. Existing deepfake detection methods either rely on developing classification methods to better fit the distributions of the training data, or exploiting forgery synthesis mechanisms to learn a more comprehensive forgery distribution. Unfortunately, these methods tend to overlook the essential role of real data knowledge, which limits their generalization ability in processing the unseen real and fake data. To tackle these challenges, in this paper, we propose a simple and novel approach, named Knowledge Injection based deepfake Detection (KID), by constructing a multi-task learning based knowledge injection framework, which can be easily plugged into existing ViT-based backbone models, including foundation models. Specifically, a knowledge injection module is proposed to learn and inject necessary knowledge into the backbone model, to achieve a more accurate modeling of the distributions of real and fake data. A coarse-grained forgery localization branch is constructed to learn the forgery locations in a multi-task learning manner, to enrich the learned forgery knowledge for the knowledge injection module. Two layer-wise suppression and contrast losses are proposed to emphasize the knowledge of real data in the knowledge injection module, to further balance the portions of the real and fake knowledge. Extensive experiments have demonstrated that our KID possesses excellent compatibility with different scales of ViT-based backbone models, and achieves state-of-the-art generalization performance while enhancing the training convergence speed.

1. Introduction

The rapid advancement of generative AI models, such as GANs [19] and VAEs [26], have significantly promoted the development of deepfake technology. Since highly realistic deepfakes (a.k.a. deep facial forgeries) can be exploited for malicious purposes, such as financial fraud [6] or political defamation [5], which tends to induce severe consequences,

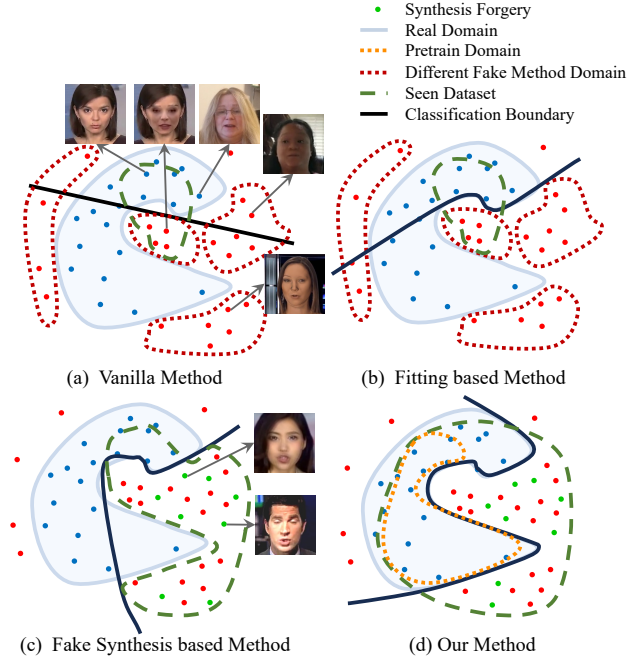


Figure 1. Biased classification boundary caused by the model’s insufficient comprehension of real or fake image distribution. The vanilla method and fitting based method are usually limited to the training set, resulting in a biased classification boundary. Fake synthesis based methods have a better understanding of fake image distribution and thus establish more effective boundaries, but still lack a robust grasp of the characteristics of real images. Our proposed approach achieves a more thorough understanding of both real and fake images.

deepfake detection becomes vital in fighting against these deepfakes. With the growing prevalence of deepfakes on social media platforms, it is imperative to develop deepfake detection methods with high generalization ability to handle the deepfakes produced by unseen generative methods.

The majority of the previous methods [8, 10, 28, 32, 37, 49] mainly rely on the learning capacity of deep neural networks (DNNs) to learn certain forgery cues from the training set, to differentiate deepfakes from real data.

Specifically, early vanilla methods [8, 37], which only utilize DNNs, directly learn the detection cues from the real and fake data, as shown in Fig. 1a. Then, the fitting based methods [13, 31, 48], which improve the vanilla method by exploiting special designs such as attention mechanism, further refine the decision boundary to better fit the distributions of the training real and fake data, as shown in Fig. 1b. Unfortunately, these methods tend to perform decently within the domain of the training data while struggling with the testing data from unseen forgery techniques. Meanwhile, fake synthesis based approaches [27, 39] generate fake training data via forgery synthesis pipelines based on prior knowledge, e.g. blending boundaries, and establish more effective decision boundaries, as shown in Fig. 1c. Although these methods enable the backbone DNNs to learn a more comprehensive forgery distribution, they have not paid enough attentions to the distribution of real images. Their understanding of the real data is only limited to the training data, which makes them difficult to process the unseen real data. Therefore, these methods can hardly establish an accurate classification boundary, which is simultaneously correlated to the distributions of both the real and deepfake data, to differentiate the unseen deepfakes from the real data.

To overcome the aforementioned issues, in this paper, we propose a novel approach, named Knowledge Injection based deepfake Detection (KID). Specifically, we propose a multi-task learning based Knowledge Injection framework, which contains a knowledge injection module, a coarse-grained forgery localization branch and two layer-wise suppression and contrast losses (S&C). To preserve the real data knowledge in the pre-trained backbone model obtained from the pre-training stage while integrating the understanding of deepfake data, we propose a knowledge injection module to progressively learn the distributions of real and fake data, and inject the learned knowledge into the backbone model. To constrain the knowledge injection module to learn more forgery cues and enhance the location-awareness of injected forgery knowledge, we construct a coarse-grained forgery localization branch by capturing the consistency across regions in real images and the inconsistencies within fake images. To emphasize the knowledge of real data to balance the portions of real and fake knowledge, we propose two layer-wise suppression and contrast losses. The entire framework also utilizes self-blended images [11] as the training fake data to boost the model’s capacity to generalize across unseen deepfake techniques. In general, the framework can simultaneously learn the distributions of real and fake data and learn more generalized fake features, to establish a more accurate classification boundary for unseen real and fake data.

Our major contributions are summarized as follows:

- We propose a novel deepfake detection method, named

Knowledge Injection based deepfake Detection (KID), by constructing a multi-task learning based knowledge injection framework, which can be easily plugged into existing ViT-based models, including foundation models.

- We propose a knowledge injection module to preserve the knowledge of real data while injecting the understanding of deepfake data into the backbone model, to enable a more accurate modeling of the distributions of real and fake data.
- We construct a coarse-grained forgery localization branch to enrich the learned forgery knowledge, including the forgery locations, in a multi-task learning manner.
- We propose two layer-wise suppression and contrast losses to constrain the knowledge injection module, to emphasize the knowledge of real data to further balance the portions of real and fake knowledge.
- Extensive experiments have demonstrated that Our KID possesses excellent compatibility with different scales of ViT-based backbone models, and achieves state-of-the-art generalization performance while enhancing the training convergence speed.

2. Related Work

In recent years, deepfake detection techniques have been continuously evolving. Early biometric based methods primarily concentrated on heuristic features, such as head pose [46], eye blinking [29], and optical flow [9], etc. However, these approaches usually struggle to remain effective when processing high-quality deepfake data.

Meanwhile, early vanilla methods [8, 37], which only utilize DNNs, directly learned the detection cues from the real and fake data, and drew massive attentions from researchers. Then, researchers quickly started to focus on improving the learning ability of DNNs, and numerous subsequent methods have been developed. From the perspective of training mechanism, these methods can be primarily classified into two categories, fitting based methods [8, 36, 37, 48] and fake synthesis based methods [11, 17, 27, 39].

2.1. Fitting based Method

Among the fitting based methods, some of them [13, 48] introduce attention mechanism to highlight suspicious regions in fake images. Meanwhile, methods like SPSL [31] and F3-Net [36] explore the frequency domain to identify forged content, which is not obvious in the spatial domain. Other techniques, such as PCL [49] and PD [47], compare real and fake segments within the image to reveal inconsistencies. Despite these advances, these fitting-based methods primarily focus on differentiating real and fake data with cues learned from the training data, which makes them less effective against unseen data.

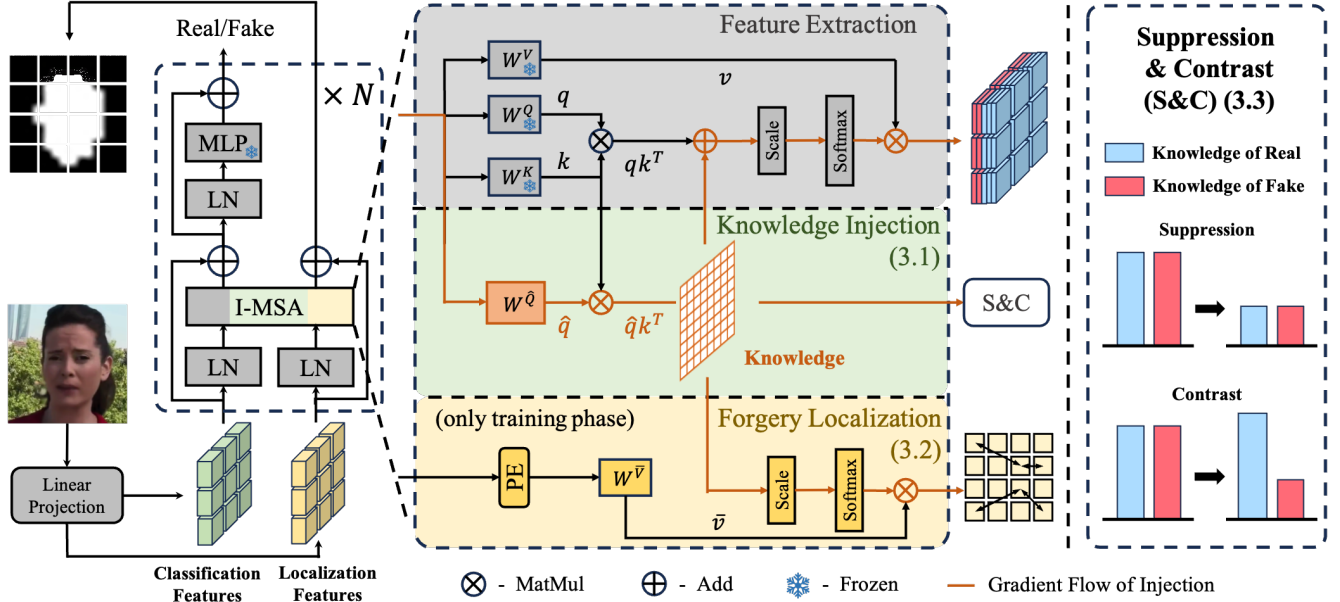


Figure 2. Overview of the Knowledge Injection based deepfake Detection framework.

2.2. Fake Synthesis based Method

By recognizing the limitations of fitting based methods, researchers also explored generating fake images via forgery synthesis pipelines, to help the detection model to learn a more general knowledge from the fake training data. Then, the fake synthesis based methods became less overfitted to the training data and deepfake techniques. Face X-ray [27] firstly proposed to swap faces with similar facial landmarks and enable the detection model to focus on the blending boundaries. Then, ICT [17] exploited this mechanism to help its identity learning and SLADD [11] provided more diverse editing content. SBI [39] further improved the forgery synthesis mechanisms by creating more realistic fake images with diverse forgery types, in a self-blending manner. These methods can learn a more general distribution of the fake data and establish a more effective decision boundary.

While these fake synthesis methods focus on improving the generalization ability of handling unseen fake data, they usually overlook the importance of the real data distributions, which makes them difficult to process the unseen real data. To address this issue, based on the strengths of fake data synthesis, we further capture a more precise representation of real and fake data distributions to better handle unseen data, via our proposed knowledge injection framework, which is compatible with ViT-based DNN models (including foundation models). With our proposed method, we provide a new direction for handling emerging deepfakes and enhancing the generalization ability to fight against the unseen deepfake techniques.

3. Methodology

Existing forgery detection methods usually overlook the role of real images, leading to imprecise classification boundaries and making it difficult to distinguish unseen real and fake data. To address these challenges, we propose the Knowledge Injection based deepfake Detection (KID) method by constructing a multi-task learning based knowledge injection framework. Our framework comprises three main components: a knowledge injection module, a coarse-grained forgery localization branch, and two layer-wise suppression and contrast losses, as illustrated in Fig. 2. By leveraging these components along with a ViT-based backbone model and the self-blended training fake data, our KID can effectively learn the distributions of both real and fake images and establish a more precise classification boundary to distinguish the unseen real and fake images. Note that in this section we employ ViT [18] as an example backbone model for convenience.

3.1. Knowledge Injection Module

Since the employed ViT-based pre-trained model has been trained on the pre-training datasets such as ImageNet, which only contains real images, the backbone model naturally possesses extensive knowledge about the distribution of real images. This motivates us to propose our knowledge injection module, to preserve the knowledge of real data in the pre-trained backbone model while injecting the understandings of deepfake data.

The ViT-based pre-trained models have shown remarkable performances in many classification tasks including

deepfake detection, which can be attributed to their core attention mechanism. To integrate our knowledge injection framework into the backbone model, we propose an Injection Multi-Head Self-Attention (I-MSA) block to replace the regular multi-head self-attention block to perform knowledge injection.

Let P_l represent the input features of the I-MSA block at the l -th layer. P_l is firstly splitted into multi-head features, denoted as H_l^i . In addition to the standard QKV (Query, Key, Value) calculations, we introduce an additional knowledge query vector, \bar{Q} , to calculate the authenticity correlation between image patches as

$$\bar{Q} = H_l^i W_l^{\bar{Q}}. \quad (1)$$

The authenticity correlation matrix \overline{Corr}_l , which represents the learned knowledge about the distributions of real and fake data, is then calculated based on \bar{Q} and the key vector K , as

$$\overline{Corr}_l^i = \frac{\bar{Q}_l^i K_l^i}{\sqrt{d_k}}. \quad (2)$$

After the computation of the detection-related knowledge, it is further injected into the features obtained from the standard QKV calculations. Then, the self-attention is calculated as Eq. (3), by utilizing the injected features to complete the feature update

$$head_l^i = \text{softmax}\left(\frac{Q_l^i K_l^i}{\sqrt{d_k}} + \overline{Corr}_l^i\right) V_l^i. \quad (3)$$

Via the adoption of the knowledge injection module, our KID can preserve the knowledge of real data learned by the backbone network, and obtain a more general representation of the real data distribution. Meanwhile, the module also acquire the knowledge of fake data distribution with the help of our coarse-grained forgery localization branch. Constrained by our layer-wise suppression and contrast losses, the knowledge injection module can acquire a more general knowledge of the authenticity-related cues and inject this knowledge into the backbone model to improve the modeling of both the real and fake data.

In the training process, the original attention branch is frozen and only the weight matrix $W_l^{\bar{Q}}$ is updated. The gradient flow in the I-MSA block is denoted by the orange-colored path in Fig. 2. Under such circumstance, our framework can significantly reduce the amount of parameters to be updated, which simplifies the learning of the knowledge injection module, to achieve a faster convergence speed compared to the full-parameter tuning.

3.2. Coarse-Grained Forgery Localization Branch

To guide the knowledge injection module in learning the knowledge of fake data and enhance the location-awareness

of the injected knowledge, we construct a separate coarse-grained forgery localization branch, as shown in Fig. 2. Different from the original classification branch, our localization branch provides a supplementary pathway to constrain the detection model in a multi-task learning manner.

Before the processing of the transformer blocks, the initial localization features are obtained via identical approach as the initial classification features but with separate parameters. Once the auxiliary localization features L_l are fed into the I-MSA block, Positional Encoding(PE) is applied to enhance the perception of positional information.

During the update process, the localization features L_{l+1} is finally updated based on the knowledge authenticity correlation matrix, as

$$L_{l+1} = \text{softmax}(\overline{Corr}_l) \cdot \text{LN}(L_l + PE) \cdot W_l^{\bar{K}}. \quad (4)$$

Since the primary goal of our method is deepfake detection rather than accurate forgery localization, no upsampling operation is performed at the output of the entire network to avoid additional computations. Instead, a MLP layer is constructed to conduct coarse-grained classifications on the output image patch features of the last layer.

The corresponding coarse-grained localization ground truth is calculated based on the percentage Γ_i of the number of pixels belonging to the outer face within each patch. The label of the i -th patch y_i is defined as

$$y_i = \begin{cases} 0, & \Gamma_i < \gamma_0 \\ 1, & \Gamma_i > \gamma_1 \\ \Gamma_i, & \text{otherwise} \end{cases}, \quad (5)$$

where γ_0 and γ_1 are hyperparameters which stand for the thresholds. For each patch, the percentage of the number of pixels belonging to the outer face Γ_i within each patch is compared to these thresholds to label the patch as either an inner face patch or an outer face patch. Otherwise, the label is directly assigned based on the value of Γ_i , which represents the boundary region.

At last, a dice loss is calculated to update the coarse-grained forgery localization branch. With the coarse-grained forgery localization branch, the knowledge injection module can better perceive spatial information and characterize the distribution of fake data.

Remark. Eq. (3) can be reformed to

$$head_l^i = \text{softmax}\left(\frac{H_l^i (W_l^Q + W_l^{\bar{Q}}) K_l^i}{\sqrt{d_k}}\right) V_l^i. \quad (6)$$

Apparently, W_l^Q and $W_l^{\bar{Q}}$ are symmetric. Then,

$$\frac{\partial L_{CE}}{\partial W_l^Q} = \frac{\partial L_{CE}}{\partial W_l^{\bar{Q}}}, \quad (7)$$

where L_{CE} represents the cross-entropy loss. This observation implies that if the backbone network only incorporates the knowledge injection module, its training process is actually equivalent to updating the parameter W_l^Q of a ViT model to fit the training set. Then, the detection model behaves similarly to a fitting-based method. By incorporating the coarse-grained forgery localization branch, we can disrupt this symmetry and constrain the knowledge injection module to concentrate on learning the forgery cues.

3.3. Layer-Wise Suppression and Contrast Losses

With the help of the coarse-grained forgery localization branch, the detection model can concentrate on learning the forgery cues. However, without a proper constraint for the knowledge learning process, the detection model may over-emphasize the knowledge of fake data and can hardly balance the learned knowledge of the real and fake data. Under such circumstance, the detection model may still overfit to certain specific characteristics of the training set and then hurt the generalization ability.

To reasonably emphasize the knowledge of real data within the knowledge injection module and further balance the contributions of real and fake knowledge, we propose two layer-wise suppression and contrast losses. Unlike the coarse-grained forgery localization branch, our layer-wise suppression and contrast losses provide fine-grained control across each layer, to properly constrain the knowledge learned by the knowledge injection module.

Specifically, we suppress the activation values in the authenticity correlation matrix at the shallow layers, as described in Eq. (8) and Eq. (9). This suppression loss constrains the detection model to maintain the core understandings of real data distributions at the shallow layers

$$A_l = \frac{1}{MN} \sum_{i=0}^M \sum_{j=0}^N |\overline{Corr_{l,i,j}}|, \quad (8)$$

$$L_S = \sum_{l=0}^{L_0} \frac{\sum_{b=0}^B \max(0, A_l - \beta)}{B}. \quad (9)$$

Note that A_l calculates the averaged activation value of the authenticity correlation matrix $\overline{Corr_l}$, which measures the extent of knowledge (modifications) to be injected to the features extracted from the backbone model. Meanwhile, to allow the knowledge injection module to still learn the necessary knowledge for effective deepfake detection, we introduce an upper limit parameter β to prevent excessive suppression. Then, the suppression loss L_S is computed as the sum of losses across layers $0 - L_0$.

At deep layers, the suppression loss will not be utilized and the contrast loss will be applied. According to general observations, real images generally exhibit strong internal consistencies and correlations across patches, whereas fake

images often display inconsistencies between manipulated and benign regions, due to the imperfections of deepfake techniques. Therefore, we formulate the contrast loss based on the above intuitions, as

$$L_D = \sum_{l=L-2}^L \frac{\sum_{b=0}^B \max(0, A_l^{fake} - A_l^{real} + \mu)}{B}, \quad (10)$$

where A_l^{real} and A_l^{fake} represent the activation values for the deep layers corresponding to the real and fake images, respectively. Note that μ is a hyperparameter that sets the minimum acceptable difference between the activation values of real and fake images. During the training process, the contrast loss is computed based on the authenticity correlation matrices (knowledge) from the I-MSA blocks in the final two transformer blocks. By applying the contrast loss, the detection model effectively improves the knowledge of the distributions of real and fake images, and thus establishes a more accurate classification boundary.

3.4. Overall Loss

At last, the overall loss function of our KID, as shown in Eq. (11), is formed by integrating the cross entropy loss of the deepfake classification, the dice loss for coarse-grained forgery localization branch, and the layer-wise suppression and contrast losses. Note that the entire coarse-grained forgery localization branch is only utilized in the training phase.

$$L = L_{CE} + L_{DICE} + L_S + L_D \quad (11)$$

4. Experiments

4.1. Experimental Settings

Datasets. Following the settings used in [11], we adopt the FF++ [37] as the training set. The dataset contains 1,000 real images and 4,000 fake images generated by four manipulation methods: Deepfakes (DF) [2], Face2Face (F2F) [43], FaceSwap (FS) [1], and NeuralTextures (NT) [44]. To assess the generalization ability and stability of the training model across different datasets, we also conduct tests on four additional datasets: Celeb-DF-v2(CDF) [30], DeepFakeDetection(DFD) [3], DeepFake Detection Challenge public test set(DFDC) [4] and Wild-Deepfake(FFIW) [51]. These alternative datasets contain a greater number and higher quality of fake images, providing a robust platform for evaluating the model’s performance.

Evaluation Metrics. To thoroughly verify the generalization ability of our method and compare its performance with previous methods, we adopt the evaluation protocol from [11], we utilize the area under the receiver operating characteristic curve(AUC) as the primary evaluation metric, following [11].

Methods	Input Type	Training Set			Test Set AUC(%)			
		Real	Fake	DFD	CDF	DFDC	FFIW	
LipForensics [22]	Video	✓	✓	-	82.40	73.50	-	
FTCN [50]	Video	✓	✓	94.40	86.90	71.00	74.47	
FInfer [23]	Video	✓	✓	-	70.60	-	69.46	
FADE [41]	Video	✓	✓	96.23	77.46	-	-	
AltFreezing [45]	Video	✓	✓	98.50	89.50	-	-	
ViT [18]	Frame	✓	✓	89.75	73.49	69.90	-	
Face X-ray [27]	Frame	✓	✓	93.47	-	-	-	
PCL+I2G [49]	Frame	✓	✗	99.07	90.03	67.52	-	
ICT [17]	Frame	✓	✗	84.13	85.71	-	-	
DCL [40]	Frame	✓	✗	91.66	82.30	-	71.14	
SBI+Xception [39]	Frame	✓	✗	97.56	93.18	72.42	76.72	
AUNet [10]	Frame	✓	✗	<u>99.22</u>	92.77	<u>73.82</u>	<u>81.45</u>	
IID [25]	Frame	✓	✓	93.92	83.80	-	-	
IIL [16]	Frame	✓	✓	99.03	93.88	-	-	
LAA-Net [34]	Frame	✓	✗	98.43	<u>95.40</u>	-	80.03	
KID (Ours)	Frame	✓	✗	99.46	95.74	75.77	82.53	

Table 1. **Cross-dataset** evaluation in terms of AUC on DFD, CDF, DFDC and FFIW. The results of prior methods are directly cited from the original paper for a fair comparison. Bold and underlined values correspond to the best and the second-best values, respectively. Our method outperforms the state-of-the-art methods on all four datasets.

Implementation details. Throughout the experiment, RetinaFace [15] is used to detect the facial region, which is then cropped, and aligned, and the images are saved as input with the size of 224×224 . We adopt ViT/B-16 [18] pre-trained on ImageNet [14] as the model backbone. In the training stage, the model is trained for a maximum of 300 epochs using the AdamW optimizer [33], with a weight decay of 0.01 and a batch size of 24. Early stopping is implemented, terminating training when the loss doesn't decrease for 20 consecutive epochs. The initial learning rate is set to 1×10^{-4} , and we utilize cosine annealing for learning rate decay, with a lower bound of 1×10^{-6} . The only updated parameters of the backbone part are class token and normalization layers. For data augmentation, we apply horizontal flipping, random hue saturation changes, random brightness contrast changes, JPEG compression, blurring and SBI [11] fake synthesis. The upper and lower bounds in Eq. (5) are defined as $\gamma_0 = 0.2$ and $\gamma_1 = 0.8$. Additionally, the boundary parameters in Eq. (9) and Eq. (10) are set to $\beta = 1.2$ and $\mu = 0.1$. In the inference stage, we randomly extract 32 frames from each video for detection and take the average of the frame-level results as the video-level result. All experiments are conducted on four RTX 3080 Ti GPUs.

4.2. Cross-Dataset Evaluation

To demonstrate the superiority of our method in terms of generalizability, we evaluate the performance of our model, trained on the FF++ dataset, across various datasets and

Methods	Test Set AUC(%)	
	FF++	CDF
Xception [12]	99.70	65.30
EN-B4 [42]	99.22	66.24
MAT [48]	99.80	76.65
F^3 -Net [36]	98.10	65.17
Face X-ray [27]	98.52	74.20
SPSL [31]	96.91	76.88
DCL [40]	99.30	81.00
SLADD [11]	98.40	79.70
IID [25]	99.32	82.04
GS [21]	99.95	84.97
KID (Ours)	98.91	86.32

Table 2. **Cross-dataset** evaluation for single-frame images without context on the CDF dataset by training on FF++.

compare it to previous methods. The results are shown in Tab. 1.

Comparison with Frame-Level Methods. We first compare our method with the frame-level detection methods. Our method achieves state-of-the-art performance on all four datasets, outperforming the second-best result by 1.86%, 1.95% and 1.08% on the high-quality forgery datasets Celeb-DF (CDF), DFDC and FFIW, respectively. The results indicate that our proposed method has supe-

Method	Test Set AUC(%)				
	DF	F2F	FS	NT	FF++
X-ray [27]	99.17	98.57	98.21	98.13	98.52
PCL+I2G [49]	100.00	98.97	99.86	97.63	99.11
SBI [39]	99.99	99.90	98.79	98.20	99.22
AUNet [10]	99.98	99.60	99.89	<u>98.38</u>	<u>99.46</u>
KID (Ours)	100.00	<u>99.87</u>	<u>99.81</u>	98.47	99.59

Table 3. Cross-manipulation evaluation on FF++ dataset. All forgery methods are unseen during training.

rior generalization and detection capabilities when faced with unknown, high-quality fake data. Additionally, certain methods only detect single-frame images without providing video-level results. For comparison with some frame-level methods, Tab. 2 shows the performance of our method against existing single-frame detection techniques on the CDF dataset. While our approach is slightly outperformed by MAT on the FF++ dataset, likely because it does not utilize fake images from FF++, it achieves the highest performance on CDF. This result demonstrates that our method performs at a cutting-edge level for single-image detection, even without relying on contextual information.

Comparison with Video-Level Methods. We then compare our method with various video-level detection methods. These methods typically require consecutive frames as input and leverage temporal correlation for detection. As shown in Tab. 1, even when randomly selecting frames, our method achieves the best performance, surpassing the state-of-the-art by 6.24% and 4.77% on the CDF and DFDC datasets, respectively. These results confirm that our method retains strong generalization performance without relying on temporal information.

4.3. Cross-Manipulation Evaluation

In deepfake detection tasks, not only the original images and post-forgery processing are critical, but the forgery technique itself also has a significant impact on forgery outcomes. To evaluate the model’s robustness across different methods, we tested the detection performance of our proposed method on various manipulation techniques.

Tab. 3 shows the performance of our method when tested on four manipulation methods present in the FF++ dataset. Since synthetic fake data is used during training, these four manipulation methods are unseen to the model. According to the results, our method achieves the best performance on the DF and NT forgery techniques, as well as overall. Moreover, the proposed method secures the second-best performance on F2F and FS methods, with only marginal differences of 0.03% (F2F) and 0.08% (FS) from the best results. These results demonstrate the excellent generalization capability of the proposed method across various manipulation

KIM	SBI	CGFLB	S&C	Test Set AUC(%)			
				FF++	DFD	CDF	DFDC
✗	✗	✗	✗	96.36	82.78	73.49	61.55
✓	✗	✗	✗	98.93	96.77	87.35	70.94
✓	✓	✗	✗	96.11	98.06	89.72	72.03
✓	✓	✓	✗	98.84	98.04	91.49	74.05
✓	✓	✓	✓	99.59	99.46	95.74	75.77

Table 4. The effect of key components of our KID. KIM (3.1), CGFLB (3.2) and S&C (3.3) refer to the three key components of our method.

Method	Test Set AUC(%)				
	FF++	DFD	CDF	DFDC	Avg
ViT w/o KI	96.36	82.78	73.49	61.55	78.55
ViT w/ KI	99.59	99.46	95.74	77.57	93.09
DinoV2 w/o KI	98.66	96.87	78.83	65.95	85.08
DinoV2 w/ KI	99.73	99.31	82.70	72.98	88.68
LeViT w/o KI	95.49	92.57	72.10	60.86	80.25
LeViT w/ KI	97.20	93.16	79.75	67.25	84.34

Table 5. Generalization performances of different pre-trained transformer models with and without the knowledge inject framework.

methods.

4.4. Ablation Study

Effect of Each Component. We conduct quantitative experiments on the three key components of our method and the SBI [11] method used in the training process to evaluate the contribution of each part. The experimental results are presented in Tab. 4. As shown in the table, it is evident that each of the three proposed components contributes significantly to the model’s performance across all four test datasets. When all components are integrated, the model achieves the best overall performance. Specifically, the knowledge injection module (3.1) plays the most crucial role, improving the model’s performance by an average of 9.95% while the coarse-grained forgery localization branch (3.2) and the layer-wise suppression and contrast losses (3.3) also contribute significantly to overall effectiveness.

Impact on the Pre-trained Models. We also apply the knowledge injection framework to the ViT-based backbone models DinoV2 [35] and the more lightweight LeViT [20]. The experimental results, as shown in Tab. 5, demonstrate that the proposed framework knowledge injection framework possesses excellent compatibility with various ViT-based backbone models across multiple scales.

Furthermore, we analyze the impact of the knowledge

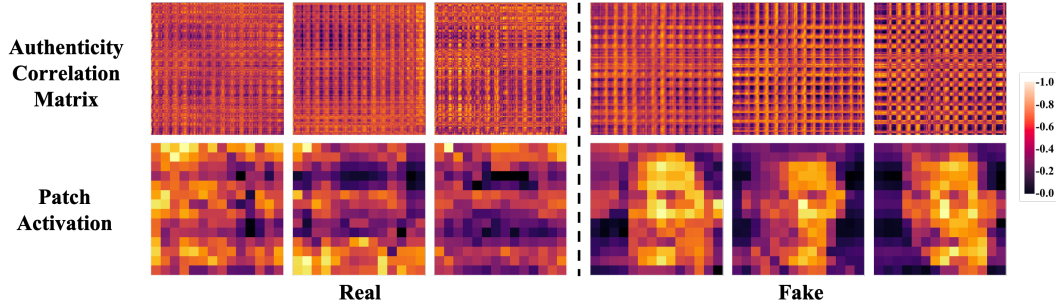


Figure 3. Visualization of the authenticity correlation matrix in Eq. (3). The Patch Activation in the second row represents the average correlation between each patch and all other patches in the matrix.

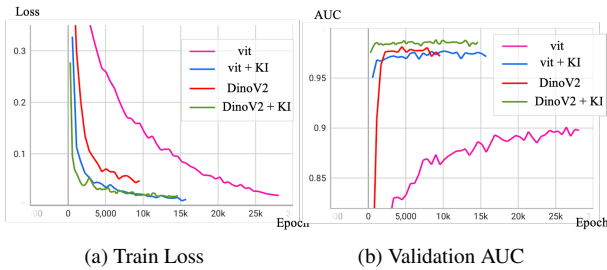


Figure 4. Training loss and validation AUC curves of different pre-trained models after incorporating the knowledge injection framework.

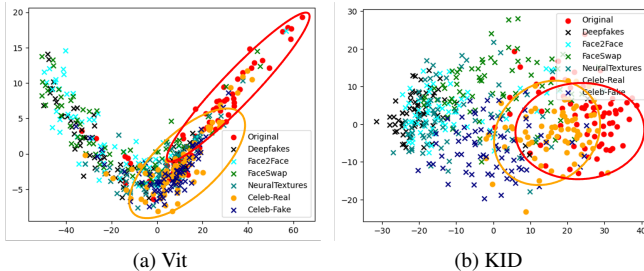


Figure 5. The PCA feature spaces visualization of the basic ViT(a) and KID(b). The dots represent real images, the crosses represent forged images, and different colors represent different forgery methods in CDF and FF++ test sets. The circles represent the boundaries of real image features within and across domains. Best viewed in color.

injection framework on the training process, as illustrated in Fig. 4. With the knowledge injection framework incorporated, the model converges faster (4x faster for ViT, 2x faster for DinoV2) and exhibits better performance on both training and validation sets. This demonstrates that the knowledge injection framework effectively enhances model training efficiency and performance, highlighting its compatibility with ViT and DinoV2.

4.5. Qualitative Analysis

Knowledge Visualization. In Fig. 3, we visualize the learned knowledge as described in Eq. (3). The real images exhibit an average correlation due to the inherent consistency, while the fake images display significant periodic fluctuations, reflecting distinct regions with different distributions. We further obtain patch activation by averaging correlations across patches. The activation reveal high internal correlation in swapped areas of fake images and low correlation elsewhere, whereas real images show no such pattern. This demonstrates that the learned knowledge effectively aids in distinguishing real from fake images.

Feature Space. We perform PCA [7] dimensionality reduction on the final layer features of the test set images extracted by the model to observe the learned feature space, as shown in Fig. 5. While the baseline model effectively differentiates real images within the training set, it struggles with distinguishing real images across domains from fake ones. In contrast, KID exhibits more accurate classification boundaries and more consistent distributions of real images across datasets, despite some overlap between high-quality forgeries and the real domain for CDF and NT. This highlights the improved representation of both real and fake images.

5. Conclusion

In this paper, we observe that existing deepfake detection methods usually overlook the learned knowledge of real data, which limits their generalization ability to handle the unseen real and fake images. To address this issue, we propose a simple yet novel method named Knowledge Injection based deepfake Detection (KID), by constructing a multi-task learning knowledge injection framework that is compatible with ViT-based backbone models. In the proposed framework, we propose a knowledge injection module to improve the model’s understandings of the distributions of real and fake data, via injecting specifically learned knowledge to the backbone network. We construct a coarse-grained forgery localization branch to enrich the forgery knowledge learned by the knowledge

injection module. We propose two layer-wise suppression and contrast losses to balance the learned knowledge of real and fake data. Extensive experiments demonstrate that our KID achieves state-of-the-art generalization performances and faster convergence speed, and our framework is compatible with ViT, DinoV2 and LeViT.

References

- [1] Faceswap. <https://github.com/MarekKowalski/FaceSwap>, 2016. Accessed: 2024-10-16. 5
- [2] Deepfakes. <https://www.github.com/deepfakes/faceswap>, 2017. Accessed: 2024-10-16. 5
- [3] Contributing data to deepfake detection research. <https://ai.googleblog.com/2019/09/contributing-data-to-deepfake-detection.html>, 2019. Accessed: 2022-04-09. 5
- [4] Deepfake detection challenge. <https://www.kaggle.com/c/deepfake-detection-challenge>, 2019. Accessed: 2024-10-16. 5
- [5] Deepfake video of zelenskyy could be 'tip of the iceberg' in info war, experts warn. <https://www.npr.org/2022/03/16/1087062648/deepfake-video-zelenskyy-experts-war-manipulation-ukraine-russia>, 2022. Accessed: 2024-10-16. 1
- [6] Finance worker pays out 25 million after video call with deepfake 'chief financial officer'. <https://edition.cnn.com/2024/02/04/asia/deepfake-cfo-scam-hong-kong-intl-hnk/index.html>, 2022. Accessed: 2024-10-16. 1
- [7] Hervé Abdi and Lynne J Williams. Principal component analysis. *Wiley interdisciplinary reviews: computational statistics*, 2(4):433–459, 2010. 8
- [8] D. Afchar, V. Nozick, J. Yamagishi, and I. Echizen. Mesonet: a compact facial video forgery detection network. In *IEEE WIFS*, pages 1–7, 2018. 1, 2
- [9] Irene Amerini, Leonardo Galteri, Roberto Caldelli, and Alberto Del Bimbo. Deepfake video detection through optical flow based cnn. In *Proceedings of the IEEE/CVF International Conference on Computer Vision Workshops*, pages 0–0, 2019. 2
- [10] Weiming Bai, Yufan Liu, Zhipeng Zhang, Bing Li, and Weiming Hu. Aunet: Learning relations between action units for face forgery detection. In *Proceedings of the IEEE/CVF Conference on Computer Vision and Pattern Recognition*, pages 24709–24719, 2023. 1, 6, 7
- [11] Liang Chen, Yong Zhang, Yibing Song, Lingqiao Liu, and Jue Wang. Self-supervised learning of adversarial example: Towards good generalizations for deepfake detection. In *Proceedings of the IEEE/CVF Conference on Computer Vision and Pattern Recognition*, pages 18710–18719, 2022. 2, 3, 5, 6, 7
- [12] F. Chollet. Xception: Deep learning with depthwise separable convolutions. In *Proceedings of the IEEE/CVF Conference on Computer Vision and Pattern Recognition*, pages 1251–1258, 2017. 6
- [13] Hao Dang, Feng Liu, Joel Stehouwer, Xiaoming Liu, and Anil K Jain. On the detection of digital face manipulation. In *Proceedings of the IEEE/CVF Conference on Computer Vision and Pattern Recognition*, pages 5781–5790, 2020. 2
- [14] Jia Deng, Wei Dong, Richard Socher, Li-Jia Li, Kai Li, and Li Fei-Fei. Imagenet: A large-scale hierarchical image database. In *Proceedings of the IEEE/CVF Conference on Computer Vision and Pattern Recognition*, pages 248–255, 2009. 6
- [15] Jiankang Deng, Jia Guo, Yuxiang Zhou, Jinke Yu, Irene Kotsia, and Stefanos Zafeiriou. Retinaface: Single-stage dense face localisation in the wild. *arXiv preprint arXiv:1905.00641*, 2019. 6
- [16] Shichao Dong, Jin Wang, Renhe Ji, Jiajun Liang, Haoqiang Fan, and Zheng Ge. Implicit identity leakage: The stumbling block to improving deepfake detection generalization. In *Proceedings of the IEEE/CVF Conference on Computer Vision and Pattern Recognition*, pages 3994–4004, 2023. 6
- [17] X. Dong, J. Bao, D. Chen, T. Zhang, W. Zhang, N. Yu, D. Chen, F. Wen, and B. Guo. Protecting celebrities from deepfake with identity consistency transformer. In *Proceedings of the IEEE/CVF Conference on Computer Vision and Pattern Recognition*, pages 9468–9478, 2022. 2, 3, 6
- [18] Alexey Dosovitskiy. An image is worth 16x16 words: Transformers for image recognition at scale. *arXiv preprint arXiv:2010.11929*, 2020. 3, 6
- [19] I. Goodfellow, J. Pouget-Abadie, M. Mirza, B. Xu, D. Warde-Farley, S. Ozair, A. Courville, and Y. Bengio. Generative adversarial nets. In *Advances in Neural Information Processing Systems*, pages 2672–2680. 1
- [20] B Graham et al. Levit: a vision transformer in convnet's clothing for faster inference. In *ICCV*, 2021. 7
- [21] Ying Guo, Cheng Zhen, and Pengfei Yan. Controllable guide-space for generalizable face forgery detection. In *Proceedings of the IEEE/CVF International Conference on Computer Vision*, pages 20818–20827, 2023. 6
- [22] Alexandros Haliassos, Konstantinos Vougioukas, Stavros Petridis, and Maja Pantic. Lips don't lie: A generalisable and robust approach to face forgery detection. In *Proceedings of the IEEE/CVF Conference on Computer Vision and Pattern Recognition*, pages 5039–5049, 2021. 6
- [23] Juan Hu, Xin Liao, Jinwen Liang, Wenbo Zhou, and Zheng Qin. Finfer: Frame inference-based deepfake detection for high-visual-quality videos. In *Proceedings of the AAAI Conference on Artificial Intelligence*, pages 951–959, 2022. 6
- [24] E J Hu et al. Lora: Low-rank adaptation of large language models. In *ICLR*, 2022. 1
- [25] Baojin Huang, Zhongyuan Wang, Jifan Yang, Jiaxin Ai, Qin Zou, Qian Wang, and Dengpan Ye. Implicit identity driven deepfake face swapping detection. In *Proceedings of the IEEE/CVF Conference on Computer Vision and Pattern Recognition*, pages 4490–4499, 2023. 6
- [26] D. P. Kingma and M. Welling. Auto-encoding variational bayes. *arXiv preprint arXiv:1312.6114*, 2013. 1

- [27] L. Li, J. Bao, T. Zhang, H. Yang, D. Chen, F. Wen, and B. Guo. Face x-ray for more general face forgery detection. In *Proceedings of the IEEE/CVF Conference on Computer Vision and Pattern Recognition*, pages 5001–5010, 2020. [2](#), [3](#), [6](#), [7](#)
- [28] Y. Li and S. Lyu. Exposing deepfake videos by detecting face warping artifacts. *arXiv preprint arXiv:1811.00656*, 2018. [1](#)
- [29] Y. Li, M. C. Chang, and S. Lyu. In ictu oculi: Exposing ai created fake videos by detecting eye blinking. In *IEEE International Workshop on Information Forensics and Security*, pages 1–7. IEEE, 2018. [2](#)
- [30] Y. Li, X. Yang, P. Sun, H. Qi, and S. Lyu. Celeb-df: A large-scale challenging dataset for deepfake forensics. In *Proceedings of the IEEE/CVF Conference on Computer Vision and Pattern Recognition*, pages 3207–3216, 2020. [5](#)
- [31] H. Liu, X. Li, W. Zhou, Y. Chen, Y. He, H. Xue, W. Zhang, and N. Yu. Spatial-phase shallow learning: rethinking face forgery detection in frequency domain. In *Proceedings of the IEEE/CVF Conference on Computer Vision and Pattern Recognition*, pages 772–781, 2021. [2](#), [6](#)
- [32] Z. Liu, X. Qi, and P. H. Torr. Global texture enhancement for fake face detection in the wild. In *Proceedings of the IEEE/CVF Conference on Computer Vision and Pattern Recognition*, pages 8060–8069, 2020. [1](#)
- [33] I Loshchilov. Decoupled weight decay regularization. *arXiv preprint arXiv:1711.05101*, 2017. [6](#)
- [34] D Nguyen et al. Laa-net: Localized artifact attention network for quality-agnostic and generalizable deepfake detection. In *CVPR*, 2024. [6](#)
- [35] Maxime Oquab, Timothée Darcet, Théo Moutakanni, Huy Vo, Marc Szafraniec, Vasil Khalidov, Pierre Fernandez, Daniel Haziza, Francisco Massa, Alaaeldin El-Nouby, et al. Dinov2: Learning robust visual features without supervision. *arXiv preprint arXiv:2304.07193*, 2023. [7](#)
- [36] Y. Qian, G. Yin, L. Sheng, Z. Chen, and J. Shao. Thinking in frequency: Face forgery detection by mining frequency-aware clues. In *European Conference on Computer Vision*, pages 86–103. Springer, 2020. [2](#), [6](#)
- [37] A. Rossler, D. Cozzolino, L. Verdoliva, C. Riess, J. Thies, and M. Nießner. Faceforensics++: Learning to detect manipulated facial images. In *Proceedings of the IEEE/CVF International Conference on Computer Vision*, pages 1–11, 2019. [1](#), [2](#), [5](#)
- [38] Ramprasaath R Selvaraju, Michael Cogswell, Abhishek Das, Ramakrishna Vedantam, Devi Parikh, and Dhruv Batra. Grad-cam: Visual explanations from deep networks via gradient-based localization. In *Proceedings of the IEEE/CVF International Conference on Computer Vision*, pages 618–626, 2017. [1](#), [2](#)
- [39] Kaede Shiohara and Toshihiko Yamasaki. Detecting deepfakes with self-blended images. In *Proceedings of the IEEE/CVF Conference on Computer Vision and Pattern Recognition*, pages 18720–18729, 2022. [2](#), [3](#), [6](#), [7](#)
- [40] Ke Sun, Taiping Yao, Shen Chen, Shouhong Ding, Jilin Li, and Rongrong Ji. Dual contrastive learning for general face forgery detection. In *Proceedings of the AAAI Conference on Artificial Intelligence*, pages 2316–2324, 2022. [6](#)
- [41] Lingfeng Tan, Yunhong Wang, Junfu Wang, Liang Yang, Xunxun Chen, and Yuanfang Guo. Deepfake video detection via facial action dependencies estimation. In *Proceedings of the AAAI Conference on Artificial Intelligence*, pages 5276–5284, 2023. [6](#)
- [42] M. Tan and Q. Le. Efficientnet: Rethinking model scaling for convolutional neural networks. In *Proceedings of the International Conference on Machine Learning*, pages 6105–6114. PMLR, 2019. [6](#)
- [43] Justus Thies, Michael Zollhofer, Marc Stamminger, Christian Theobalt, and Matthias Nießner. Face2face: Real-time face capture and reenactment of rgb videos. In *Proceedings of the IEEE/CVF Conference on Computer Vision and Pattern Recognition*, pages 2387–2395, 2016. [5](#)
- [44] Justus Thies, Michael Zollhofer, and Matthias Nießner. Deferred neural rendering: Image synthesis using neural textures. *Acm Transactions on Graphics (TOG)*, 38(4):1–12, 2019. [5](#)
- [45] Zhendong Wang, Jianmin Bao, Wengang Zhou, Weilun Wang, and Houqiang Li. Altfreezing for more general video face forgery detection. In *Proceedings of the IEEE/CVF Conference on Computer Vision and Pattern Recognition*, pages 4129–4138, 2023. [6](#)
- [46] X. Yang, Y. Li, and S. Lyu. Exposing deep fakes using inconsistent head poses. In *IEEE International Conference on Acoustics, Speech and Signal Processing*, pages 8261–8265, 2019. [2](#)
- [47] B. Zhang, S. Li, G. Feng, Z. Qian, and X. Zhang. Patch diffusion: A general module for face manipulation detection. In *Proceedings of the AAAI Conference on Artificial Intelligence*, 36(3):3243–3251, 2022. [2](#)
- [48] H. Zhao, W. Zhou, D. Chen, T. Wei, W. Zhang, and N. Yu. Multi-attentional deepfake detection. In *Proceedings of the IEEE/CVF Conference on Computer Vision and Pattern Recognition*, pages 2185–2194, 2021. [2](#), [6](#)
- [49] Tianchen Zhao, Xiang Xu, Mingze Xu, Hui Ding, Yuanjun Xiong, and Wei Xia. Learning self-consistency for deepfake detection. In *Proceedings of the IEEE/CVF International Conference on Computer Vision*, pages 15023–15033, 2021. [1](#), [2](#), [6](#), [7](#)
- [50] Yinglin Zheng, Jianmin Bao, Dong Chen, Ming Zeng, and Fang Wen. Exploring temporal coherence for more general video face forgery detection. In *Proceedings of the IEEE/CVF International Conference on Computer Vision*, pages 15044–15054, 2021. [6](#)
- [51] Tianfei Zhou, Wenguan Wang, Zhiyuan Liang, and Jianbing Shen. Face forensics in the wild. In *Proceedings of the IEEE/CVF Conference on Computer Vision and Pattern Recognition*, pages 5778–5788, 2021. [5](#)

Deepfake Detection via Knowledge Injection

Supplementary Material

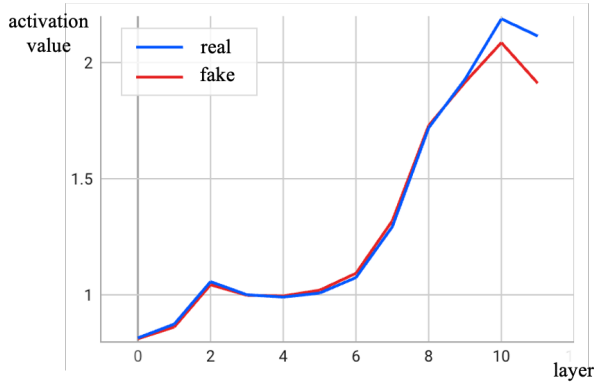


Figure A1. Layer-wise activation value of injection knowledge.

Methods	Test Set AUC(%)		
	DFD	CDF	FFIW
Vit + LoRA [24]	94.80	85.48	67.30
KID (Ours)	99.46	95.74	82.53

Table A1. Comparison with LoRA.

A. Layer-wise Injection Analysis

To explore the differences in the knowledge of real and fake images learned by the model, we computed the activation value of each layer’s authenticity correlation matrix in the model, following Eq. (8). The results are displayed in Fig. A1. Specifically, shallow layers inject less knowledge, preserving more fundamental representations of real data distributions. In contrast, deep layers learn more distinctions of the inconsistencies between real and fake data, resulting in more pronounced differences in the learned knowledge. These findings are consistent with the conclusions presented in Sec. 3.3.

B. Saliency Map.

In Fig. A3, we present GradCAM [38] visualization comparison between the SBI method and our proposed method, along with the coarse-grained localization results of our approach. Compared to CNN-based SBI methods, our approach places greater emphasis on key areas like the eyes and mouth, extracting richer information from more scattered and detailed facial regions. The localization results demonstrate that our coarse-grained forged localization branch can exploit knowledge to perform coarse localization tasks, allowing the knowledge injection module to

β	μ	Test Set AUC(%)		
		DFD	CDF	DFDC
1.0	0.1	<u>99.00</u>	95.86	72.87
1.5	0.1	98.37	93.53	70.66
1.2	0.05	97.45	93.99	71.12
1.2	0.2	98.80	95.46	<u>74.22</u>
1.2	0.1	99.46	<u>95.74</u>	75.77

Table A2. The impact of the hyper-parameters β and μ .

learn more location information during training.

C. Hyper-parameter Ablation Study

We conduct ablation experiments on the β and μ hyperparameters in Layer-Wise Suppression and Contrast Losses to evaluate their impact on model performance. As shown in Tab. A2, the overly strict restrictions on shallow layers hinder the model’s learning ability, reducing generalization performance, while excessively loose restrictions lead to overfitting. For contrast loss in deeper layers, a smaller limit μ diminishes the model’s ability to distinguish between real and fake images, while a higher limit μ , though less deviating from optimal performance, causes the model to overemphasize the differences, making it harder to converge to an optimal solution. Based on the above experiments, we selected $\beta = 1.2$ and $\mu = 0.1$ for our final model configuration.

D. KID v.s. LoRA

Since both LoRA[24] and the knowledge injection framework in this paper perform branch-based partial fine-tuning for downstream generalization, we compare our proposed KID method with LoRA in the context of deepfake detection. As shown in Tab. A1, our method significantly outperforms LoRA in terms of generalization, demonstrating that our approach leverages knowledge more effectively through multiple learning strategies in deepfake detection tasks.

E. Robustness Experiments

To assess the robustness of our method, we compare the performance with other approaches under various image degradation scenarios. The experiment involves five common degradation strategies: JPEG compression, saturation change, Gaussian blur, Gaussian noise, and contrast change. As shown in Fig. A2, while all methods experience varying

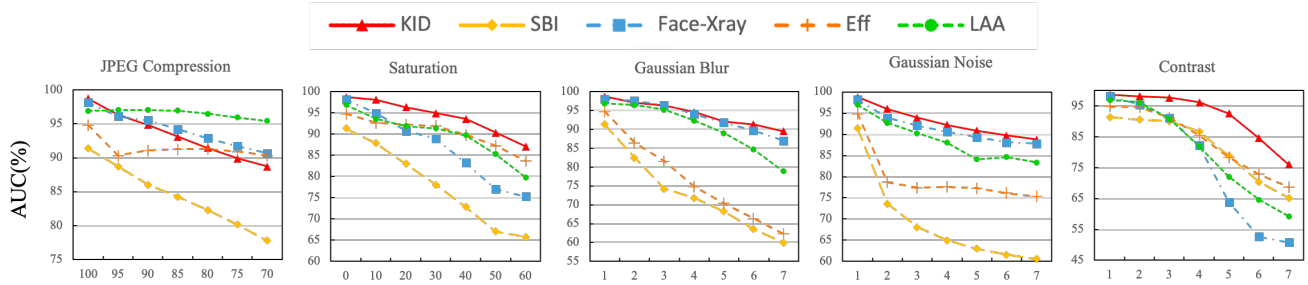


Figure A2. Robustness to different image degradation.

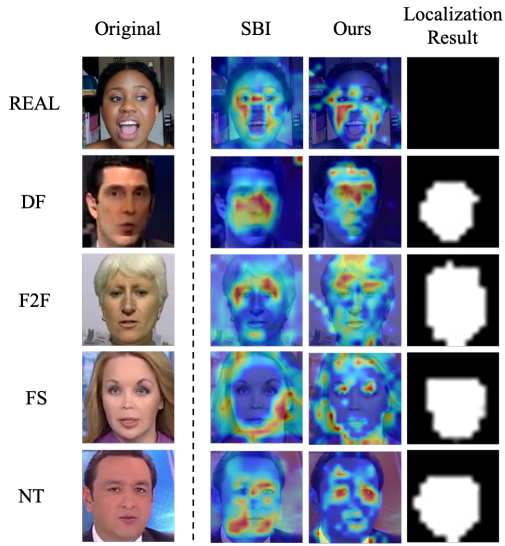


Figure A3. GradCAM [38] visualization of images from different methods in the FF++ dataset and coarse-grained localization results.

degrees of performance degradation as the image quality deteriorates, our method consistently maintains high detection accuracy. This demonstrates that our approach is resilient to different post-processing effects, making it well-suited for real-world forgery detection tasks.